



Gas-solid conversion of lignin to carboxylic acids

Journal:	<i>Reaction Chemistry & Engineering</i>
Manuscript ID	RE-ART-03-2016-000053.R1
Article Type:	Paper
Date Submitted by the Author:	17-Apr-2016
Complete List of Authors:	Lotfi, Samira; Ecole polytechnique de Montreal, Chemical engineering Boffito, Daria Camilla; Polytechnique Montreal , Chemical Engineering Patience, Gregory; Polytechnique Montreal, Chemical Engineering

Cite this: DOI: 10.1039/xxxxxxxxxx

Gas-solid conversion of lignin to carboxylic acids

Samira Lotfi,^{*a}, Daria C. Boffito and Gregory S. Patience^bReceived Date
Accepted Date

DOI: 10.1039/xxxxxxxxxx

www.rsc.org/journalname

Lignin represents 15 % to 40 % of the dry weight of lignocellulosic biomass but remains under exploited as a sustainable feedstock for chemical and fuels even though it is the only bio-polymer with aromatic units. Technology that **selectively** converts lignin to value added specialties would improve the economics of the burgeoning bio-refinery industry. Here, we introduce a two stage gas-phase catalytic process that produces carboxylic acids and aromatics from lignin while minimizing coke and char and maintaining catalyst activity. In the first step, a mixture of 50 % water vapour in air crack and partially oxidize this complex macromolecule (< 550 °C). The effluent gas contacts heterogeneous mixed-metal oxides or metal catalysts in the second step. The product profile from the second step included aromatic compounds but mostly C₄ carboxylic acids such as maleic acid and butyric acid. Vanadium catalysts cleave lignin bonds, open aromatic rings and oxidize lignin to carboxylic acids, especially maleic acid. WO₃/TiO₂ mostly gave butyric acid. Basic catalysts produced more aromatic compounds. The maximum amount of coke was 5 % of the total carbon in lignin.

1 Introduction

Bio-refineries that convert lignocellulosic biomass into fuels and chemicals represent a paradigm shift versus the pulp and paper industry that dominates the market. Lignocellulosics contains cellulose, hemicellulose and lignin macromolecules.¹ Cellulose and hemicellulose are raw materials for bioethanol, bio-butane and other chemicals.^{2–4} The pulp and paper industry combusts as much as 40 % of their lignin. Only 2 % is converted to value-added chemicals³ and the rest is waste — 50 million tons per year.^{2,5} **According to 2007 U.S. Energy Security and Independence Act, 79 Mm³ of biofuels from biomass generates 62 million tons of lignin as a residue.**³

Methoxylated phenylpropane units linked by C–C and ether bonds constitute the skeleton of lignin as a bio-polymer.² Lignin accounts for 15 % to 40 % of lignocellulose, but the heterogeneity of its structure converts it to an uncommon feedstock for chemicals or even liquid fuels.^{6,7} Moreover, process requires a homogeneous feedstock to minimize multiple purification trains that engender costs and complexity for biorefiners.^{2,6}

Pyrolysis, gasification, hydrogenation, oxidation, aqueous reforming, hydrolysis and enzymatic processes convert lignin to aromatic compounds.^{1,2,8–10} The products include low molecular weight phenolic compounds, carboxylic acids and quinones. Depolymerization of lignin leads to fuels rather than chemicals

and includes a complex mixture of molecules. **Oxidative cleavage of lignin mainly yields polyfunctional aromatic compounds including aromatic aldehydes and carboxylic acids.**¹¹

The market for aromatic acids and aldehydes is smaller, while the market for ring-opened, high purity aliphatic acids is much larger and includes pharmaceuticals, food, petrochemicals and polymers.^{3,5,6} **One of the challenges of the oxidative cleavage of lignin is to limit the further oxidation of the liquid products of interest to gas.**¹²

Heterogeneous catalysis plays a key role in the manufacture of polymers, agricultural and pharmaceuticals, especially in selective oxidation and hydrogenation.^{13–16} Catalysts improve the selectivity to target molecules and **reduce** the activation energy so that the process operates at lower temperature. Developing a selective catalytic process to convert lignin to chemicals and fuel represents a paradigm shift with respect to current practice in the pulp and paper industry¹⁷ and could ensure the economic viability of biorefineries. **Several catalytic systems have been designed for lignin model compounds that are ineffective for real biomass substrates. For example, Pd/C depolymerises up to 98 % of dimeric lignin model compounds, but not real lignin.**¹⁸ Lignin forms coke and char and other compounds that deactivate catalysts.^{2,19}

Catalysts for oxidative cleavage of lignin include organometallic catalysts, metal-free organic catalysts, acid and base catalysts, metal salt catalysts, photo- and electro catalysts.¹¹ H₂O₂ and chalcopyrite-CuFeS₂ in an acetic acid buffer oxidized lignin to malonic, succinic, malic and maleic acid at 333 K. Ma et al. propose a molecular pathway where HO⁺ initiates the ring hydroxy-

^a 2900, Boul. Édouard-Montpetit, Montréal, Canada. Fax: +1 514 340 4059; Tel: +1 514 340 4711; E-mail: samira.lotfi@polymtl.ca.

^b 2900, Boul. Édouard-Montpetit, Montréal, Canada. Fax: +1 514 340 4059; Tel: +1 514 340 4711; E-mail: gregory-s.patience@polymtl.ca.

lation to depolymerize lignin. The reaction also produced aromatic compounds — benzoic acid, vanillin and vanillic acid. Further oxidation yields p- and o-quinone, which can undergo ring opening to give C₄ acids such as maleic, fumaric and muconic acid. Hydrolyzing these acids gave stable endpoint acids (malonic, succinic, malic and trace of maleic acid).¹⁷ Vardon *et al.*⁶ produced adipic acid from lignin model compounds. First, fed-batch biological cultivation process converted the model compound to *cis-cis* muconate acid. Then PdC catalyst hydrogenated the recovered acid to adipic acid.

Olcese *et al.*²⁰ improved the quality of lignin pyrolysis bio-oil by hydrotreating the vapours over iron-silica (Fe/SiO₂) and iron-activated carbon (Fe/AC) catalysts in a fixed bed at 400 °C and 1 bar. The products were benzene, toluene, xylenes, phenol, cresols, and alkyl phenols. Coke plugged the micropores of Fe/AC but not the mesopores of the Fe/SiO₂.²⁰

Fan *et al.*² converted lignin to ethylbenzene in a two-step process. In the first step, zeolites depolymerized lignin to aromatics (mainly benzene). In the second step, HZSM-5 (with ethanol) selectively alkylated the aromatic compounds to ethylbenzene. Large pores reduced the benzene selectivity and yield of benzene, toluene, and xylenes increased with catalyst acidity. The catalyst deactivated after 3 uses: the selectivity to benzene dropped from 23 % to 7 % but a 4 h oxygen treatment restored the original catalytic activity.² Alternating reaction/regeneration cycles is a successful strategy to maintain catalyst activity overtime and reduce deactivation.²¹

Lignin pyrolysis yields phenolic compounds that are char precursors.²² Here, we introduce a new reactor configuration that includes thermo-oxidative cracking of lignin in the gas phase, followed by catalytic oxidation in a gas-solids catalytic reactor. The products are fine chemicals, particularly carboxylic acids. To reduce the susceptibility of coking and thus reducing the regeneration cycles, we developed four micro-reactor configurations to activate lignin involving air, steam and heterogeneous catalysts. Based on screening tests, passing the effluent gases after a thermo-oxidative steam cracking step produced the mostly organic acids and phenolic compounds.

2 Experimental

2.1 Materials and catalyst preparation

2.1.1 Lignin

FPInnovations (Quebec, Canada) supplied softwood kraft lignin for all the experiments. It was recovered with the LignoForce System from the Resolute Forest Products mill in Thunder Bay (Ontario). The softwood kraft lignin had a mass fraction of 66.9 % carbon, 5.2 % hydrogen, 0.1 % nitrogen, 25.4 % oxygen, with 92 % total solids. The impurities were <0.05 % Na, 1.4 % S and 1.5 % sugar.^{21,23,24} Total solids of the Thunder Bay softwood black liquor (unwashed lignin) was 29 %. The main solid components were lignin (43 %) and NaOH (32 %). The unwashed lignin had a mass fraction of 40 % carbon, 4 % hydrogen, 0.1 % nitrogen, 35 % oxygen.

We identified the structural signature of the softwood kraft lignin by ¹³C NMR, which identifies most of the carbon groups

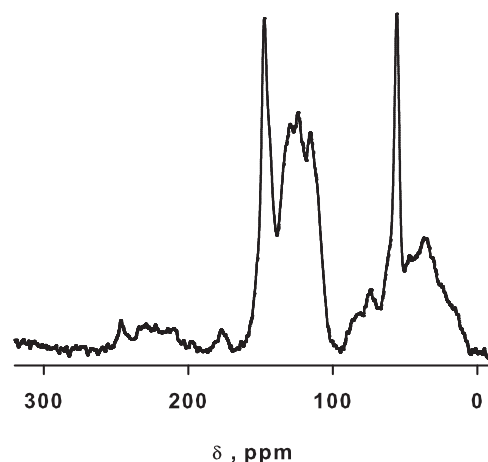


Fig. 1 ¹³C solid NMR spectrometer of Lignin

making up lignin²⁵ while other methods can also quantify the functional groups.²⁶ Most of the contributions identified belong to the β-O-4 type of linkage that characterize up to 50 % of softwood lignin. The spectral region from 185 to 164 ppm represents the C(O)O-(H,R) groups of carboxylic acids and esters.²⁷ The sharp peak at δ=147 ppm belongs to C-4 in etherified guaiacyl (G) units and C-3 in non etherified G units (β-O-4 type). Resonances at ~115 and ~127 ppm belongs to carbons 3/5 (m) and 2/6 (o) and signals between 157 and 152 ppm to the quaternary carbons in p-position.²⁸ Signal at ~87 and ~83 ppm belong to G units and represent C-α in the β-5 linkage and C-β in the β-O-4 linkage, respectively. Signals at 71.8 and 71.2 ppm still belong to G units and correspond to C-α in β-O-4 linkages and C-γ in β-β linkages. The sharp peak at δ=55.6 ppm identifies C in Ar-OCH₃.²⁹ Peaks from 53 to 49 ppm represent CH₂O of esters.²⁵ Signals from 49 to 5 ppm belongs to CH, CH₂, CH₃ aliphatic unbound with an oxygen atom. (Figure1)

2.1.2 Catalysts

In a first set of experiments, vanadium pyrophosphate (VPP) converted lignin to carboxylic acid in four reactor configurations. DuPont designed VPP to partially oxidize n-butane to MA.³⁰ In a second set of experiments, we selected the reactor configuration *iii* and tested 8 supported metal and mixed-metal oxides (Figure 2c).

- C1: V-Mo/Al₂O₃²¹
- C2: V-Mo/TiO₂
- C3: V₂O₅/MnO₂
- C4: MgO (Sigma-Aldrich — we did not purify it further)
- C5: Mg-K (Pingxiang Xingfeng Chemical Packing Co., Ltd³¹)
- C6: WO₃/TiO₂^{32,33}

- C7: V–Mo/ZSM-5
- C8: V–W/ZSM-5

C1: We impregnated γ -alumina (specific surface area (SSA) = $140 \text{ m}^2 \text{ g}^{-1}$) with V–Mo. The details are described in ²¹.

C2: We impregnated a commercial TiO_2 -IV with the metal salts and followed the same procedure as in C1 but we replaced Al_2O_3 with TiO_2 .

C3: To synthesize $\text{V}_2\text{O}_5/\text{MnO}_2$ we added 1 g of MnO_2 -IV powder to the aqueous ammonium metavanadate (1.3 g) and ammonium hydroxide (0.07 g) solution at 80°C .³⁴ After impregnation, a rotary evaporator removed most of the water at 500 mmHg and 85°C . The powder dried at 100°C and atmospheric pressure for 12 h. A static air muffle furnace calcined the $\text{V}_2\text{O}_5/\text{MnO}_2$ sample at 500°C for 6 h.

C7: We impregnated HZSM-5 with V and Mo salts and followed the same procedure as C1 but replaced Al_2O_3 with ZSM-5.

C8: For V–W/ZSM-5 we impregnated HZSM-5 with salts of V and W: 10% W and 30% V.

The catalyst reagents included: HCl (Fischer Scientific, 37%), ammonium molybdate(VI) tetrahydrate (Acros, 99%), sodium tetraborate decahydrate (Fisher Scientific, 99.5%), sodium phosphate (Sigma-Aldrich, 96%), ammonium metavanadate (ACS reagent grade, $\geq 99\%$), V_2O_5 (99.6%). The supports were HZSM-5 (Alfa Aesar, $\text{SiO}_2/\text{Al}_2\text{O}_3$ molar ratio 50:1), Titanium(IV) oxide (Alfa Aesar, 99.5% -metals basis), activated aluminum oxide (ACROS), manganese(IV) oxide and magnesium oxide (Sigma-Aldrich). We did not further purify any reagents.

2.2 Catalyst characterization

A Quantachrom Autosorb 1 MP porosimeter measured the surface area and porosity with 21 points, following the standard multi point Brunauer-Emmet-Teller (BET) method. Prior to the test, a heated bag degassed the samples at 200°C for 3 h under vacuum.

A Philipps X'pert diffractometer with a Cu-K radiation source (1.5406 \AA) at 50 kV and 40 mA generated the diffraction patterns (XRD). The instrument operated at room temperature with an angle of incidence of 0.5° . It scanned diffraction angles between 20° and 90° with a divergence slit of 1° .

A scanning electron microscope (SEM) generated images of the catalysts. An SEM-JSM-840A (JOEL Company) energy-dispersive X-ray spectroscopy (SEM-EDX) coupled with an electronic X-ray diffraction (EDX) detector identified the principal elements in the catalytic samples.

A Perkin Elmer infrared spectrometer (FTIR) with a spectral resolution of 4 cm^{-1} scanned the lignin and reactor's residue at 16 kHz. The data were collected in the range from 4000 cm^{-1} to 600 cm^{-1} . The surface composition of the samples was investigated using attenuated total reflectance (ATR) mode.

2.3 Reactor configurations

In a first set of experiments, vanadium pyrophosphate (VPP) catalyst converted lignin to carboxylic acids in four reactor configurations in two steps. During the pyrolysis and thermo-oxidation of lignin, monomers are one of the first products but they react

further to form carbon-oxides or re-polymerize during thermo-oxidation and pyrolysis consequently. Selective oxidation of these monomers to chemicals instead of gas or solid could improve product selectivity. Accordingly, we devised four two step reactor configurations. In the first step, lignin decomposed to volatile. Coincided, these compounds reacted with the heterogeneous catalysts in the second step.

- i) lignin pyrolysis + oxidation over VPP (Figure 2a)
- ii) lignin thermo-oxidation + oxidation over VPP (Figure 2b)
- iii) lignin thermo-oxidative steamcracking + oxidation over VPP (Figure 2c)
- iv) lignin thermo-oxidative steamcracking over V–Mo/HZSM-5 + oxidation on VPP (Figure 2d)

Reactor configuration *iii* maximized the yield of carboxylic acids and therefore we selected it to assess catalyst performance — yield, conversion, selectivity, product profile - in the second set of experiments (Figure 2c). The reactor was an 8 mm ID quartz tube 600 mm long with two glass wool distributors positioned 350 mm and 500 mm from the bottom. Placing the catalyst bed near the top of the reactor minimizes product degradation.

In all the experiments we loaded 250 mg of lignin above the lower distributor and 500 mg catalyst above the top distributor. The gas contact time in the catalyst bed was 0.2 s.

Two thermocouples monitored the temperature in each zone. A syringe pump injected water into the reactor from the bottom through a 0.15 mm nozzle. Argon entered the nozzle at 22 mL min^{-1} to help atomize it into small droplets.

The mole fraction of oxygen in the feed bottle was 33% (balance Ar) at a flowrate of 38 mL min^{-1} . The temperature ramp for all experiments was:

- $15^\circ\text{C min}^{-1}$ up to 150°C
- 5°C min^{-1} up to 350°C
- 5°C min^{-1} up to 450°C , (75 min from the beginning of the reaction)
- 5°C min^{-1} up to 550°C (105 min from the beginning of the reaction)

The choice of the heating rate was dictated by TGA experiments in air, which showed that lignin lost $\sim 40\%$ of its weight above $\sim 500^\circ\text{C}$. We repeated selected tests two and three times.

2.3.1 Analytical

An ice bath trapped the condensable product from the catalyst and we sampled the liquid at each temperature step. A Hanna electrical conductivity measured the concentration of ionizable solutes present in the sample to monitor the productivity.³⁵

A Varian HPLC (Metacarb 87H column) analyzed the liquid sample offline. We calibrated the HPLC with standard solutions for each product we detected, building a calibration curve with six concentrations. We repeated each analysis three times. A Pfeiffer mass spectrometer (MS) monitored the permanent gases online.

At the end of the last temperature ramp and hold at 550 °C no solids remained above the first distributor. We calibrated the MS with a mixture of hydrocarbons and oxygen at four concentrations. The carbon balance was the sum of the carbon in the gas phase (MS) + the carbon in the liquid phase + the carbon remained on the catalyst surface. The mass of carbon remaining on the catalyst we measured by TGA. The MS detected CO, CO₂ and CH₄. We calculated the carbon trapped in the water-ice quench as the difference between the carbon loaded to the reactor and that detected on the catalyst and in the gas phase and by HPLC. We assumed that the response factors for the unknown aromatics (detected by HPLC) were the same as other known aromatics that we had previously evaluated by GC-MS²¹. These two methods differed by less than 10 %

3 Results and discussions

3.1 Two-step lignin degradation

3.1.1 Configuration i: Lignin pyrolysis + oxidation on VPP

In reactor configuration i, the lignin in the first step pyrolyzed (Figure 2a) and oxygen entered the reactor just below the second distributor. The catalyst in the second stage oxidized the pyrolysis vapours into aromatics and aliphatic carboxylic acids. Pyrolyzing lignin produces 10 % to 20 % gas and 3 % to 30 % phenolic compounds.^{36,37} The phenolic monomers can either condense to oligomers that are the precursors of char or form compounds that are precursors to fuels and chemicals by catalytic hydrogenation.³ In configuration i, the temperature breaks the β -O-4 bonds and produces the phenolic monomers in the first stage. Some of these phenolic compounds reach the second stage (VPP bed), whereas 46 % form char and remains in the lower bed. The catalyst and oxygen open the rings of the phenolic compounds and oxidize the compounds of which maleic acid was the most abundant product.

We proposed a reaction pathways to form maleic acid from lignin: the V³⁺ ion activates lignin to attract p electrons of the double bonds and generate a positive charge displaced on the ring. The ring opens by successive attack of 2O₂.²¹

Here, 19 % of the carbon in the lignin converted to liquid. The selectivity to maleic acid was 84 %. The production of light monomers during pyrolysis could account for the high maleic acid selectivity. Other products were aromatics (6 %) acrylic acid (2.6 %), malonic acid (2.6 %), followed by formic, lactic, acetic acid and vanillin. The solid residue remaining above the first distributor was the highest among the four configurations (46 %) due to the char (Table 1).

3.1.2 Configuration ii: lignin thermo-oxidation + oxidation on VPP

In configuration ii, a stream containing a mole fraction of 21 % oxygen degrades the lignin (Figure 2b). VPP oxidized the vapours formed in the first step and 36 % of the products were C₅-C₈ aromatics. The other compounds included: Maleic acid (32 %), fumaric acid (4.5 %), malonic acid (6 %), gallic acid, lactic and formic acid.

We attribute the large gas fraction produced in this configuration (73 %) to either the decarbonylation of lignin monomeric

units, lignin gasification, or to combustion of coke on the catalyst to CO and CO₂. (Table 1).

3.1.3 Configuration iii: lignin thermo-oxidative steamcracking + oxidation on VPP

In the third system, steam and oxygen cracked the lignin (Figure 2c). The vapours produced in the first step passed through the VPP and scavenged the remaining oxygen. This configuration converted the most lignin to liquid products with 48 % selectivity to maleic anhydride, 31 % to aromatics, 7 % to acrylic acid, followed by malonic, gallic and lactic acid. This configuration produced as much gas as in reactor configuration ii (Table 1).

3.1.4 Configuration iv: lignin thermo-oxidative steam cracking over V-Mo/HZSM-5 + oxidation on VPP

In the fourth configuration (Figure 2d) V-Mo/HZSM-5 and steam cracked and partially oxidized the lignin in the first step ($Q_{water}=5\text{ cm}^3\text{ min}^{-1}$ and a mole fraction of 21 % O₂). VPP partially oxidized the intermediates formed in the first step in the second step. Most of the lignin formed gas (81 %) and only 13 % was recovered in the quench including: 16 % aromatics, 47 % maleic acid, 12 % malonic acid, 10 % butyric acid, 7 % phthalic acid followed by acetic, formic acid and vanillin (Table 1).

The high cracking activity of V-Mo/HZSM-5 is responsible for the high yield of gases, as well as the combustion of the coke on the catalyst during the reaction.

Beside lignin, we tested unwashed lignin in the same condition as conf. iv. 19 %, 76 %, 5 % of carbon converted to liquid, gas and solid, respectively. MA selectivity reached up to 68 % and we detected 9 % aromatic, 5 % malonic, 1.5 % phthalic and formic acid.

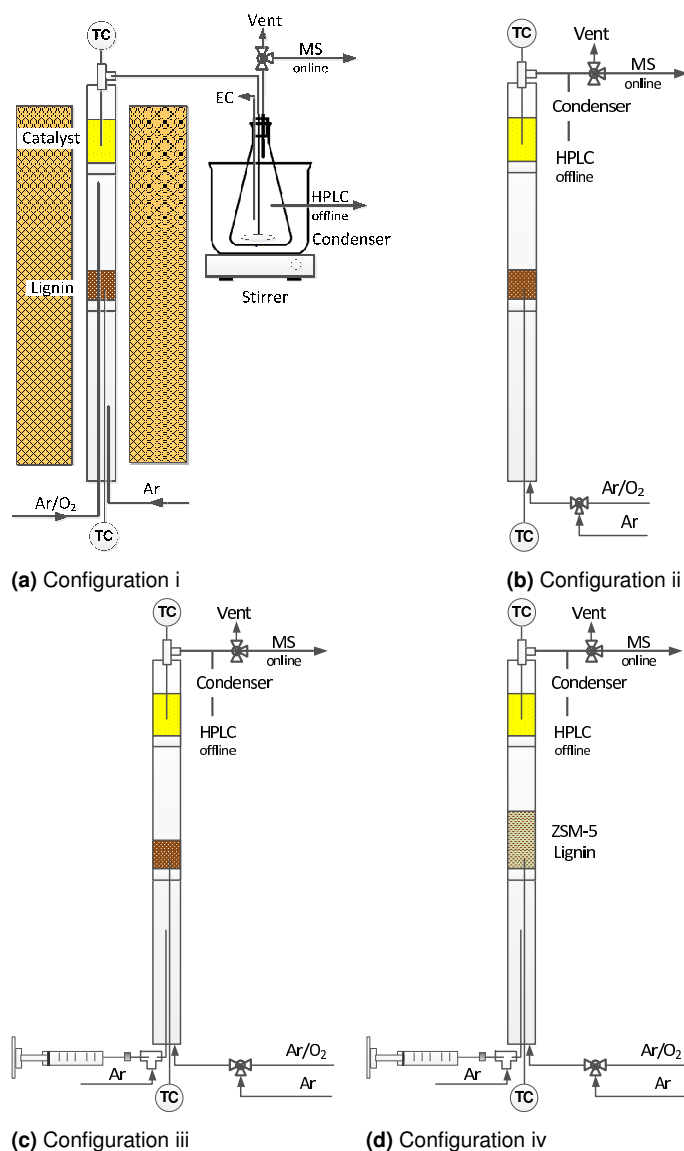


Fig. 2 Schematic of experimental setup

3.1.5 FTIR of the reaction residues

Oxidation of lignin leads to char (Figure 3b) and coke (Figure 3c).

Figure 3a FTIR spectra shows the typical lignin derivatives. Adsorption at 3420 cm^{-1} , 2944 cm^{-1} and 2833 cm^{-1} corresponds to the stretching of O-H, aromatic C-H and methoxyl groups, respectively. The bands in the range 3000 cm^{-1} to 2860 cm^{-1} correspond to the aliphatic C-H stretching, whereas the ones above 3000 cm^{-1} to the C-H aromatic stretching, which overlaps to the band of O-H. We attribute the band at 1711 cm^{-1} to the carbonyl group of aldehydes. The bands at 1520 cm^{-1} and 1594 cm^{-1} are typical of skeletal vibrations of the aromatic ring. The higher intensity of the band at 1520 cm^{-1} compared to the one at 1594 cm^{-1} is typical of softwood lignin.³⁸ C-H deformation and aromatic ring vibrations also adsorb at 1464 cm^{-1} and 1408 cm^{-1} . We attribute the bands at 1268 cm^{-1} and 1222 cm^{-1} to the C-O bonds in syringyl and guaiacyl units and the bands at 1138 cm^{-1} and 1082 cm^{-1} to the in-plane aromatic C-H deformation typical of the same com-

Table 1 Selectivity vs. reactor configuration

Name	Config. i	Config. ii	Config. iii	Config. iv
Carbon balance, (%)				
Liquid	19	23	24	13
Solid	46	4	5	6
Gas	35	73	71	81
Liquid selectivity, (%)				
Aromatic	6	36	31	16
Maleic/Fumaric acid	84	36.5	48	48
Butyric acid	-	-	-	10
Malonic acid	3.5	6	2.7	12
Formic acid	1	0.5	0.65	0.5
Acetic acid	0.1	0.3	-	1
Lactic acid	0.2	0.8	0.8	-
Phthalic acid	0.01	0.3	0.1	7
Vanillin	✓	0.3	-	2.6
Gallic acid	0.7	1.5	1.2	-
Acrylic acid	2.6	3	7	-
Syringic acid	0.06	-	-	-
Unknown	0.8	13.5	7	1.5
Benzoquinone	0.2	1	1.2	0.6
H ₂ , %	0.6	0.2	1.3	0.7

pounds.³⁹ The band at 1036 cm^{-1} refers to the C-O stretch of the O-CH₃ and C-OH. The bands at 868 cm^{-1} and 822 cm^{-1} , respectively, may correspond to lone aryl CH wag and two-adjacent aryl CH wag, respectively. The band at 626 cm^{-1} may represent the out of plane O-H band.

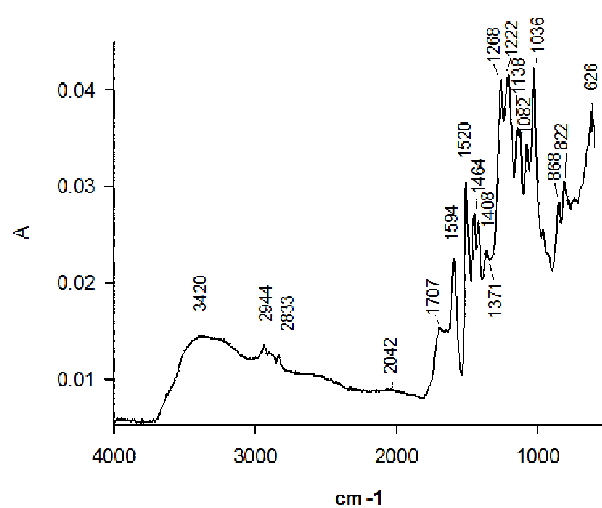
In upward shift of the FTIR spectrum baseline for most of the peaks of char remaining on the lower distributor for configuration may relate to the large carbonized compared to lignin (Figure 3b). Many typical absorption peaks of lignin disappear, in particular, the signals of the aliphatic groups. The OH-stretching band at 3390 cm^{-1} represent phenolic hydroxyl group.³⁸ C-O in carbonyl group or in carbonyl compounds conjugated with aromatic ring (1714 cm^{-1}) and aromatic ring (1590 cm^{-1}) are still present. The bands at 1160 cm^{-1} and 1088 cm^{-1} are typical of the in-plane aromatic C-H deformation of aromatic syringyl and guaiacyl units.³⁹

The FTIR spectrum of coke on V-Mo/HZSM-5 after the lignin degradation in reactor configuration iv has a typical band at $\sim 1580\text{ cm}^{-1}$ (Figure 3c). This band belongs to the highly unsaturated carbonaceous deposit called "hard coke". The bands at 1087 cm^{-1} and 870 cm^{-1} that are typical of the in-plane aromatic C-H deformation of aromatic syringyl and guaiacyl units persist.³⁹

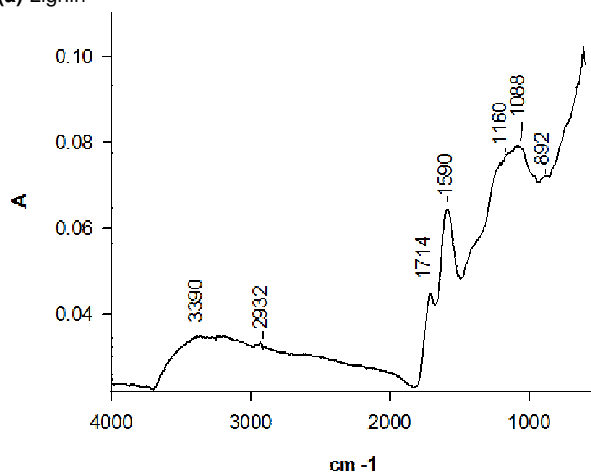
3.2 Thermo-oxidative steam cracking: catalytic activity

Besides VPP, we tested 8 other catalysts to identify the most selective towards carboxylic acids (Table 2). Metal oxides of group V and VI, like V, Mo, and W are common catalysts to partially oxidize hydrocarbons, particularly vanadium.^{40,41} Phosphoric, arsenic and boric acids control the activity of V, Mo and W in the gas phase oxidation of hydrocarbons.⁴²

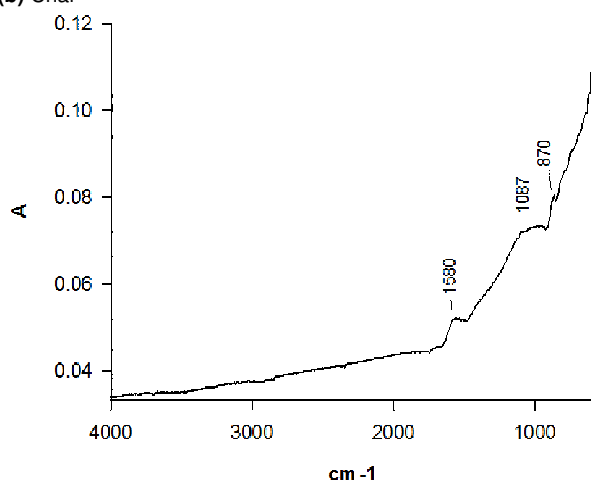
Neto *et al.*⁴⁰ designed a multi-metal oxide catalyst containing ($\text{Ag}_{a-c}\text{Q}_b\text{M}_c\text{V}_d\text{O}_e\text{eH}_2\text{O}$) to partially oxidize aromatic hydrocarbons in the gas phase to produce aldehydes, and carboxylic acids



(a) Lignin



(b) Char



(c) Coke formed during oxidation (Reaction configuration ii)

Fig. 3 FTIR spectrum

or anhydrides in fixed bed reactors.

V included in polyoxometalates catalysts degraded lignin to monomeric compounds. The catalysts comprised anionic clusters of d^0 metal cations, mostly W^{VI} , WMo^{VI} , V^V , Nb^V and oxygen anions arranged in Mo_6 octahedral units. Polymetalates cleave β -O-4 and C-C linkages of lignin and directly produce low molecular weight phenolic compounds in different oxidative environments and liquid solutions. As much as 90% of the lignin model compounds reacted.⁵ The reduction of vanadium changes with the supports and decreases as follows: $\gamma-Al_2O_3 > SiO_2-Al_2O_3 > SiO_2 > \alpha-Al_2O_3$.⁴³

The properties of the support oxide affect the activity and the selectivity of the supported metal significantly.⁴⁴ Choosing a support is as important as the choosing the oxidation catalyst.

A base such as NaOH with an extra nucleophile like NaHS, anthraquinone, acid-catalyzed hydrolysis and hydrochloric acid or $AlCl_3$ in dioxane-water or ethanol-water are all used for β -O-4 ether linkage cleavage. Lignin C-C bonds are among the most difficult bonds to break and they can also form during the lignin treatment processes. The bond is broken by fluid catalytic cracking with highly optimized zeolites in acid-catalyzed reactions.⁴⁵ The presence of sulfur in kraft lignin is a barrier in downstream catalytic processes.¹²

Though $VO_2P_2O_7$ is unequivocally the bulk compound for what we call VPP, 15 different crystalline phases may form before or during the reaction.⁴⁶ The acid sites cleave β -O-4 and α ether linkages⁴⁷ and V complexes selectively cleave C-O and C-C bonds and oxidize lignin to monomeric phenolic compounds including alcohols, aldehydes, ketones, and carboxylic acids⁵ In addition, their redox properties make them excellent catalysts for gas phase partial oxidations. Chiaregato reports that in a O_2 -rich environment, the O_2 atoms re-arranges on the VPP surface into finite δ - $VOPO_4$ domains that are the oxidation selective phase. Also polymetalates of V, Mo and W are active in the degradation of lignin to monomeric compounds. They include mostly W^{VI} , WMo^{VI} , V^V , Nb^V and oxygen anions arranged in Mo_6 octahedral units. Specifically, polymetalates cleave β -O-4 and C-C linkages of lignin, directly producing low molecular weight phenolic compounds in various solutions.⁵ We chose vanadium oxides because they carry both the strong Lewis acid and redox functionalities to cleave lignin bonds and partially oxidize it to carboxylic acids.

Ni, Co, Mo on Al_2O_3 and TiO_2 degrade lignin by oxidation, hydrogenation and hydrodeoxygenation. Commercially, catalysts combining V_2O_5 and MoO_2 partially oxidize benzene and n-butane to MA.⁴⁸ The unique catalytic properties of V and Mo is the reason why they are incorporated together in catalysts for commercial processes to oxidise and partially oxidise a wide range of compounds, including acrolein, alkanes and aromatics. We selected Mo as an active species in conjunction with V because V cycles between V^{4+} and V^{5+} , Mo cycles between Mo^{5+} and Mo^{6+} oxidation states. Mo^{5+} and Mo^{6+} are strong Lewis acids, as well as V^{4+} and V^{5+} that can therefore break lignin bonds and partially oxidize the intermediates. The V and Mo operate synergistically.⁴⁶ Differently from V and Mo, W isn't a typical oxidation catalyst, but rather activate hydration and dehydration.³³ The mechanism of lignin degradation to acrylic acid and lactic acid in-

involved hydration and de-hydration. For this reason, in C8, we supported W and V on HZSM-5.

C1: (V–Mo/Al₂O₃)

The V–Mo/Al₂O₃ catalyst partially oxidized lignin solutions (V_{O2} = 4%) to lactic acid (S=6%).²¹ Other co-products were formic acid (S=6%), acetic acid, maleic anhydride, acrylic acid and phthalic anhydride. 17% of the total carbon converted into carboxylic acids. The product distribution (Table 2) changes significantly with respect to our previous data, even if the catalyst is the same.²¹ There are 4 main differences with our previous reactor configuration in the work described herein: i) the lignin vaporized from a solid bed instead of being injected in a liquid solution into the hot catalyst ii) the catalyst does not contact pure lignin iii) the O₂ concentration is 11% vs. 4% iv) The T increased from 50 °C to ~ 500 °C whereas in the previous experiments it was constant at 370 °C.

Here, V–Mo/ Al₂O₃ converted 23% of the lignin carbon to liquids (2). The main products in the liquid were C₅–C₈ aromatic compounds (S=64%).

The second most abundant product in the quench was maleic acid (S=20%), followed by acrylic acid (S=5.5%), and lactic acid (S=5%). Vanadium and VPP in particular has a unique capacity to oxidize aromatics to maleic anhydride/acid from aromatics.^{21,49} Jongerius report that Mo reduces catalyst deactivation and improves the cleavage of the diphenylmethane bonds.⁵⁰ While the bonds involving monophenolic units split at temperatures up to 450 °C, both with and without oxygen, Mo has a role in cracking biphenyl bonds and yield phenol and benzene.⁵¹ V–Mo based catalysts oxidize o-xylene and benzene and olefins to anhydrides.⁵² Mo reduces the catalyst deactivation rate and increases cleavage of 4-hydroxydiphenyl ether, diphenyl ether, and diphenylmethane bonds.⁵⁰ Fumagalli reports that V–Mo catalysts have a high oxygen insertion capacity that oxidize the intermediates involved in the process o-xylene to phthalic anhydride.⁵³

We attribute the higher selectivity to maleic acid compared to lactic acid to the higher oxygen concentration with respect to our previous data 11% vs. 4% in²¹. Products such as formic, acetic and lactic acid form from the β-O-4 bonds cleavage at temperatures higher than 200 °C, depending on the reactivity of the substituents of the aromatic ring. The catalyst in the second stage may completely oxidize some of these acids to CO₂ and H₂O. We were unable to quantify how much H₂O the reaction produced because of the large excess of steam we co-fed with the O₂

C2: (V–Mo/TiO₂) and C7: (V–Mo/HZSM-5)

We loaded the same active components of catalyst C1 on different supports TiO₂ (C2) and HZSM-5 (C7). TiO₂ has both Lewis acid sites and basic sites that interact with high valence metal cations.⁵⁴ TiO₂ has a promoting effect as a support for vanadium oxide; in fact most commercial catalysts for o-xylene oxidation to phthalic anhydride comprise V₂O₅/TiO₂.⁵⁵ MoO₂ improves the catalytic activity of V₂O₅/TiO₂ in the oxidation of 1,2-dichlorobenzene.⁵⁶

In our case, replacing γ-Al₂O₃ with TiO₂ as a support decreased the yield of liquid to 15.5%, but increased the selectivity to maleic acid (45%). Other products were: aromatics (42%), succinic acid (7.5%), phthalic acid (7.5%), formic and acetic acid and vanillin.

Surprisingly, HZSM-5 as a support for V and Mo gave the highest selectivity to liquid products not only among the V–Mo based samples, but among all the catalysts tested. HZSM-5 zeolite is a commercial catalyst for the FCC of linear olefins and alkanes hydrocracking.⁵⁷ HZSM-5 is a strong Brønsted acid, which is desirable for the conversion of benzene to ethylbenzene, pyrolysis of biomass to liquid.^{2,58}

An hypothesis that explains the high yield of liquids relates to the very narrow pores of HZSM-5, which might be too small to host the sterically-hindered intermediates of the lignin steam cracking deriving from the first stage. The narrow pores prevent the production of those reaction intermediates that are the precursors of coke.⁵⁸ Nevertheless, the selectivity to aromatics is lower (19%) compared to C1 and C2 and maleic acid (+ fumaric acid) and butyric acid accounts for almost 40% of the selectivity to liquids. Other products are benzoic acid (8%), vanillin and phthalic acid.

C3: (V₂O₅/MnO₂)

We tested MnO₂ as a new support for vanadium. V₂O₅ selectively oxidizes o-xylene to phthalic anhydride.⁵⁹ MnO₂ is a promoter to partially oxidize methanol to formaldehyde⁶⁰ and is a support for Au in the oxidation of 5-(hydroxymethyl)furfural.⁶¹ V₂O₅/MnO₂ yields 16.5% liquid products of which the most part were aromatic compounds (36%), followed by maleic acid (18%) and butyric acid (16%). Other products were succinic and phthalic acid. The V₂O₅ most likely cracked many of the products and for this reason the selectivity towards liquids was low.⁶²

C4: (MgO)

MgO is a basic catalyst with activity towards decarbonylation and cracking.^{63,64} The oxidative steam cracking of lignin monomers over MgO produced 8.5% of liquids from lignin and more than 80% of gases. The main products were butyric acid (11%), vanillin (11%), phthalic acid (7%) and aromatics (7%). MgO may also adsorb hydrocarbons and retain them.⁶⁵ The selectivity to the solid residue was in fact the highest among all of the catalysts.

C5: (Commercial Mg–K–Si–Al catalyst)

We tested a commercial catalyst that converts benzene to maleic anhydride by Chemical Packing Co. Ltd, (China). The catalyst included Mg, Al, Si, and K (SEM-EDX analyses). The main compounds in the quench were C₅–C₈ aromatics (33%) followed by , butyric acid (33.5%), phthalic acid (7.5%), benzoic acid (15%), maleic acid, vanillin and muconic acid.

C6: (WO₃/TiO₂)

WO₃/TiO₂ dehydrates glycerol to acrolein.³³ WO₃ is active towards C–C bonds cleavage⁶⁶ and W is itself more active towards oxidation than V.⁵⁰ Moreover, W catalyzes wood hydrocracking.⁵⁰ WO₃/TiO₂ converted lignin mostly to C₄ acids, including maleic acid (9%), butyric acid (64%), phthalic acid (5%). Other products are aromatics (11%), vanillin and benzoic acid.

WO₃ has strong Lewis acid sites (W⁶⁺)^{54,67} that can activate the intermediates deriving from the lignin degradation of the first reaction stage (see the next section of reaction pathways).

Table 2 Product selectivity vs. catalyst

Name	C1	C2	C3	C4	C5	C6	C7	C8
Catalyst	V-Mo/Al ₂ O ₃	V-Mo/TiO ₂	V ₂ O ₅ /MnO ₂	MgO	Mg-Si-Al-K cat.	WO ₃ /TiO ₂	V-Mo/HZSM-5	V-W/HZSM-5
EC (μS/cm)	-	103	107	12	118	174	155	130
Carbon Balance (%)								
Liquid	23	15.5	16.5	8.5	19.5	20	25	21
Solid	6.5	4.5	3.5	11	6	4	4	7.5
Gas	70.5	80	80	80.5	74.5	76	71	71.5
Liquid selectivity (%)								
Aromatic	64	42	36	7	33.2	11	19	9.5
Maleic/Fumaric acid	20.5	45	18.5	1	1.5	9	26	56
Butyric acid	0.6	0.5	16	11	32.5	64	17	14
Malonic acid	-	-	-	-	✓	0.4	-	-
Formic acid	1	0.7	-	-	0.06	✓	-	0.1
Acetic acid	0.2	0.6	-	-	0.2	0.1	-	0.1
Lactic acid	5	-	-	-	-	-	-	-
Muconic acid	-	-	-	-	1.5	-	-	-
Succinic acid	0.8	7.5	3	-	-	-	1	8.5
Phthalic acid	0.3	2	2.5	7	7.5	5	0.5	1
Vanillin	✓	0.5	0.3	11	1.5	1.5	5	-
Benzoic acid	-	-	0.1	2.5	15	1.5	8	-
Gallic acid	0.3	-	0.15	-	✓	-	-	0.3
Acrylic acid	5.5	-	1	-	-	-	-	-
Syringic acid	0.6	-	-	-	-	-	-	-
Unknown	0.7	0.7	20	59.5	8	7	23.1	10.2
Benzoquinone	0.6	-	0.2	1	-	-	0.3	0.2
H ₂ , %	2	-	7	-	3.3	4	5.5	6

Table 3 Surface area and pore size of fresh catalysts

Catalyst	A	Pore volume
	m ² g ⁻¹	cm ³ g ⁻¹
V-Mo/Al ₂ O ₃	115	0.25
V-Mo/TiO ₂	53	-
VPP	41	0.074
V-Mo/ZSM-5	46	0.095
V-W/ZSM-5	50.7	0.124

C8: (V-W/HZSM-5)

Since W catalyzes the hydrocracking of wood⁵⁰, we replaced molybdenum with tungsten from C7 to C8. The selectivity to liquid products decreased (21% vs. 25%), but the selectivity to maleic anhydride increased from 21% to 56%). **Though WO₃ is not an oxidation catalyst, the V functionalizes this oxide.** Other products were butyric acid (14%), succinic acid (8.5%), aromatics (9.5%), formic acid, acetic acid, phthalic acid and aromatics (10%).

3.2.1 Catalyst characterization

The surface area of the V-Mo/Al₂O₃ was the highest at 115 m² g⁻¹ and the lowest was VPP at 41 m² g⁻¹ (Table 3). The pore volume of the V-Mo/Al₂O₃ was also highest at 41 cm³ g⁻¹.

The diffractogram of V-Mo/Al₂O₃ was typical of an amorphous material. The XRD pattern of V-Mo/Al₂O₃ and V-Mo/TiO₂ (Figure 4) resemble the data of Shishido et al.⁶⁸ Orthorhombic Mo₄O₁₁ crystallites and V₂O₃ form on TiO₂.⁶⁸ Peaks at 2θ = 24, 27, 33, 36, 37, 55 and 57 relates to V₂O₃ phase and peaks at 2θ = 21.8, 26, and 33.4 belongs to Mo₄O₁₁ (JCPDS 13-042).

Triclinic aluminum vanadium oxide (AlVO₄), tetragonal vanadyl molybdenum oxide (VOMoO₄), and monoclinic molybdenum vanadium oxide (Mo_{0.67}V_{0.33}O₂) forms on Al₂O₃ (Figure 4).⁶⁸

(VO)₂P₂O₁₂, (VO)₂P₂O₇, VO(PO₃)₂ and VOHPO₄·0.5H₂O phases constitute VPP (Figure 5). **As expected, (VO)₂P₂O₇ is the predominant phase, which is responsible for the catalytic activity in oxidation. VOHPO₄·0.5H₂O, which is the surface product of O₂ rearrangement in the lattice is also present.**²¹

V₂O₅ (2θ = 20, 22, 26, 31, 32, 33, 34, 39.5, 48, 52, 55, 58) and MoO₃ (2θ = 24, 26, 27, 34, 38 and 39) phases forms on HZSM-5.^{72,73} XRD detected VMO₈ and V_{0.07}Mo_{0.93} on HZSM-5

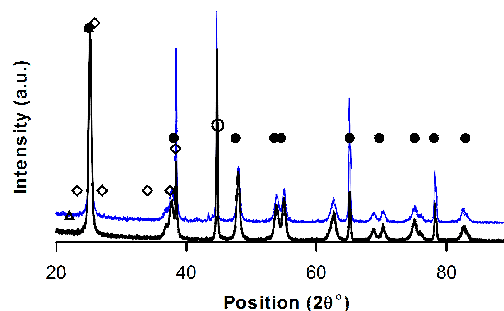


Fig. 4 XRD-V-Mo/TiO₂, ● anatase TiO₂, ◇ MoO₃, △ Mo₄V₆O₂₅, ○ VO₂⁶⁹, black = before reaction – Blue = after reaction.

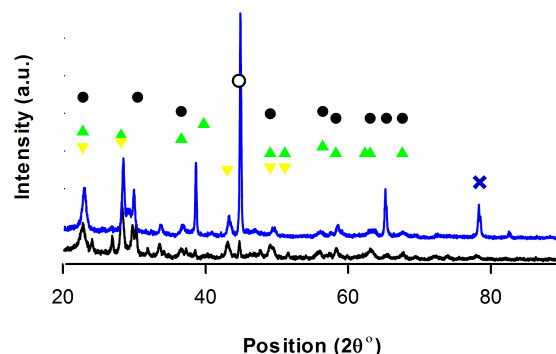


Fig. 5 XRD-VPP, ● (VO)₂P₂O₇⁷⁰, ▲ VO(PO₃)₂, △ VOHPO₄·0.5H₂O, ○ VO₂⁶⁹, × V₆O₁₃⁷¹, black = before reaction- Blue = after reaction.

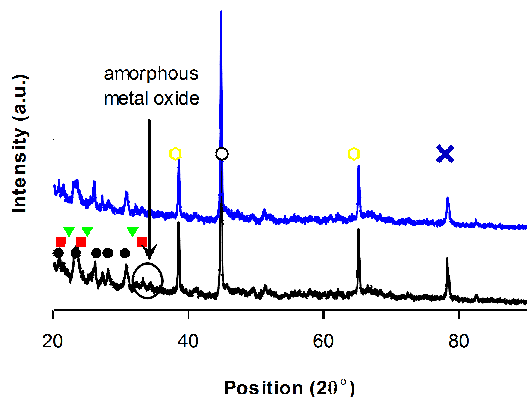


Fig. 6 XRD-V-Mo/ZSM-5, ● HZSM-5⁷⁴, ■ VMoO₈, ▼ (V_{0.07}Mo_{0.93})₅O₁₄, ○ VO₂⁶⁹, × V₆O₁₃⁷¹, □ MoO₃⁷⁵, black = before reaction- Blue = after reaction.⁷⁶

(Figure 6). These are the active V-Mo mixed oxides for oxidation reactions.⁴⁶

After the reaction, the phases detected in V-Mo/TiO₂ and V-Mo/ZSM-5 were the same as for the fresh catalyst.⁷⁷ In VPP, the intensity of the peaks at ~30 and 42 reduced. This peak belongs to monoclinic VO₂ and is observed in all XRD diffractogram of all the catalysts (Figures 5, 4, 6).⁶⁹

3.3 Discussion

3.3.1 Reactions pathways

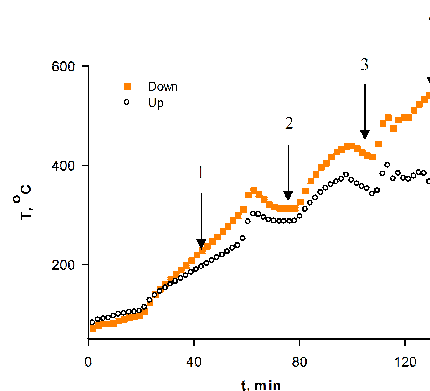
Oxidative steam-cracking lignin followed by catalytic conversion of the volatile compounds produces up to 25% liquids that includes carboxylic acids and aromatics (Table 2). Lignin begins to decompose at 200 °C and produces gases and liquids (Figures 7), which agrees with literature data.¹⁹ Maleic acid and butyric acid are among the most abundant compounds, which are easily detected by electrical conductivity.³⁵

Aromatic compounds

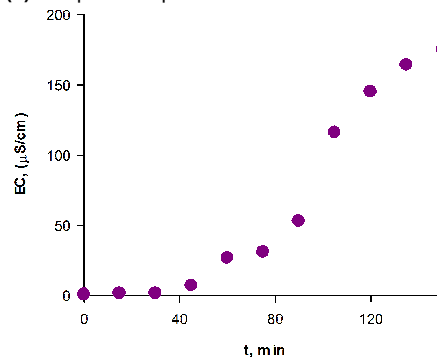
Steam and oxygen crack the lignin in the above of the lower distributor. We hypothesize that in this first step the β-O-4 bonds cleave and release the aromatic phenolic units that constitute the monomers of lignin. These units pass through the bed above the lignin or react with the catalyst to form carboxylic acids (2). The reactivity of the monomeric aromatic units depends on the type of substituents carrying oxygen functionalities.¹⁹ A GC-MS detected aromatic compounds for all the catalysts tested, in particular for the samples C1, C2, C3, C5. 1-ethyl-3-methyl cyclopentane, cyclopentane 1-ethyl-1-methyl, cyclohexane-1,4 dimethyl, ethyl benzene, benzene, 1,3-dimethyl, cyclohexane methyl, and others formed the aromatics.

Maleic and fumaric acid

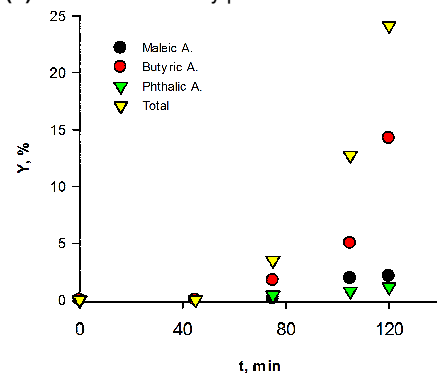
Recently, we derived a mechanism to describe how maleic an-



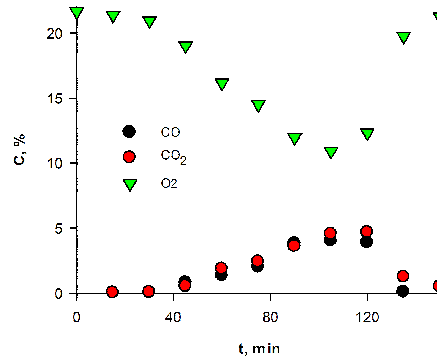
(a) Temperature profile



(b) Electro conductivity profile



(c) Liquid yield



(d) Gas

Fig. 7 WO₃/TiO₂

hydride, lactic acid, acetic acid and formic acid (and phthalic anhydride) form from pure lignin.²¹ Vanadium has a unique capacity to produce maleic anhydride/acid. V^{5+} activates the aromatic rings of the monomeric units increasing their electrophilicity, thus exposing them to the attack of 2 molecules of O_2 . After the attack of 2 O_2 the ring opens and re-arranges to maleic anhydride. Maleic anhydride hydrates to maleic acid and its isomer fumaric acid.

Butyric acid

Here for the first time we report a mechanism to account for the high concentration of butyric acid (Figure 8). We took as a representative catalyst WO_3/TiO_2 . We hypothesize that butyric acid (and crotonic acid) form from lignin in 3 steps. Step 1 includes the oxidative steam cracking of the lignin. At temperatures above 200 °C the β -O-4 bonds cleave and release the aromatic phenolic units in the reactor space above the lignin bed below the upper distributor. This rupture generates either an anion (phenolate) or a phenol radical. The negative charge or the radical will most likely displace to carbon atoms of the ring that carry an oxygen functionality to give the chetonic form.⁷⁸ In this form the carbon of the carbonyl group is strongly electrophilic and will undergo nucleophilic attack by water (steam cracking). In the attempt to recover its aromaticity, the rings open. Gierer et al. observed the same type of aromatic ring cleavage in liquid phase and presence of (H_2O_2) under both alkaline and acid conditions.⁷⁸ During step 1, O_2 might oxidize the constituents of the aromatic rings, producing carboxylic acids.²¹

Step 2 includes the activation of the intermediates formed by ring cleavage onto the catalyst. We hypothesize that the acid sites on the catalyst, either of Brønsted or Lewis type, are the active species involved in this step. WO_3 carries both strong Brønsted and Lewis acid sites. Lewis acid sites are W_6^{6+} .^{54,67} V^{5+} is a Lewis acid strong enough to activate the reaction intermediate formed during step 1. In the activation mechanism the positive charge of tungsten displaces the p electrons of the open aromatic ring, similarly as V^{5+} activates the aromatic ring after β -O-4 bonds cleavage.²¹ O_2 adds to the intermediates giving hydroxyls. The intermediate cleaves when an excess of electrons accumulate around an electrophilic carbon.

Step 3 involves hydrogen. We hypothesize that the intermediate formed during step 2 remains anchored to tungsten until hydrogen adds to it. Until the intermediate is absorbed on W it can be oxidized up to carboxylic acid, but only H_2 can displace it from the metal. Butyric acid forms after dehydration followed by hydrogenation of the crotonic acid.

Karlsson et al.^{79,80} report butyric acid derives from the ozonolysis of lignin-carbohydrate complex model compound, i.e. in strong oxidant conditions. Ozonolysis of β -O-4 structures produces erythronic and threonic acids⁸¹, which are precursors of the butanoic acid. Shao et al. report that GC-MS analyses detected butanoic acid both in a untreated liginosulfonate sample and after oxidation above $Ti/SbASnO_2$ and Ti/PbO_2 electrodes.⁸²

We hypothesized that butyric acid could form from the condensation of two molecules of acetaldehyde followed the dehydration over WO_3/TiO_2 and successive oxidation to the acid. We tested this hypothesis and fed acetaldehyde over the catalyst under the

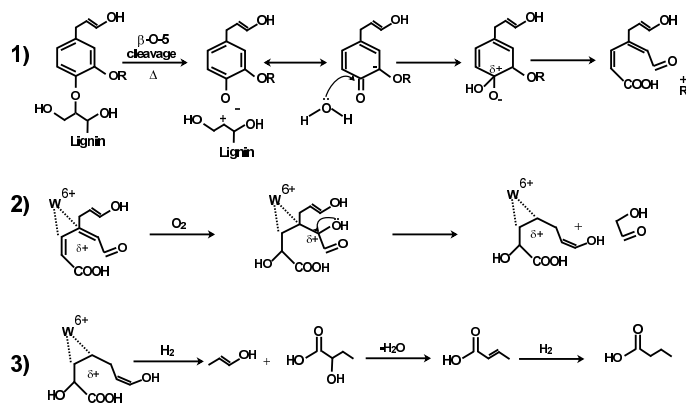


Fig. 8 Proposed Mechanism of formation of butyric acid in 3 steps.

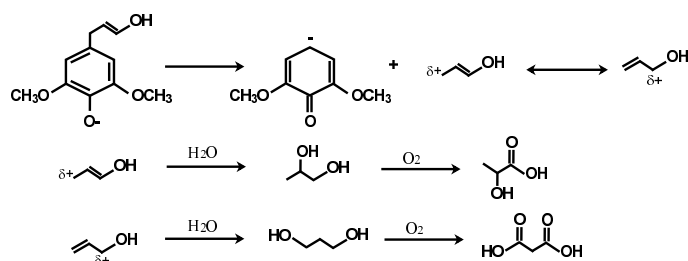


Fig. 9 Proposed mechanism of formation of lactic and malonic acids from syringyl alcohol.

same conditions but only detected acetic acid in the quench.

Lactic and malonic acids

Acrylic acid hydrates to form lactic acid.²¹ However, another possible mechanism to account for lactic acid as well as malonic acid involves cleaving propylic chains of monomeric units such as syringyl and guaiacyl (Figure 9).

Formic and acetic acid

The cleavage of methyl and ethyl constituents followed by oxidation produces formic and acetic acids.²¹

Acrylic acid

Acrylic acid may form from the scission of a phenolic unit and one of the terminal aldehydes as a consequence of the dehydration followed by oxidation.²¹ At high temperatures, lactic acid may dehydrate to acrylic acid.

Muconic acid

Muconic acid is a C_6 carboxylic acid that can form from the aromatic ring opening, followed by oxidation and dehydration.⁸³

Succinic acid

The MS detected H_2 in the gas phase which could hydrogenate maleic and fumaric acids to succinic acid. The hydrogen may form either from the gasification of lignin, which decomposes into elements (H_2 and C forming coke on the catalyst)^{21,84} or from steam reforming of the biomass into syngas ($H_2 + CO$). The concentration of succinic acid follows the same trend as that for maleic acid for the eight catalysts (Table 2): $V-Mo / TiO_2$ and $V-W / HZSM-5$ both produce the most maleic and succinic acids whereas the MgO and $MgSiAlK$ make little maleic and no succinic acid.

4 Conclusions

Lignin is an inert macromolecule and because of its heterogeneity remains underexploited commercially. Activating it with high temperatures (as in pyrolysis), oxygen and/or water vapour produces phenolic compounds and bio-oils. Catalysts can improve the selectivity to target compounds and effectively decreases the required operating temperature. Pre-mixing the lignin with catalyst increases the cracking rate but it produces more coke, char and gas. Moreover, the catalyst deactivates more rapidly. We demonstrated a two-step process in which lignin is **thermo-oxidatively steam cracked in the first step to volatile compounds which contact a catalyst bed in the second step**. Little coke formed on the catalyst (less than 5% of the total C in lignin) and the catalyst did not agglomerate.

V-Mo/Al₂O₃ and V-Mo/HZSM-5 converted 23% and 25% of the lignin into liquid products, respectively. The selectivity to maleic acid was 20% in both cases. Replacing Al₂O₃ and HZSM-5 with TiO₂ reduced the liquid yield (15.5%) but increased maleic acid selectivity (45%). Replacing molybdenum with tungsten in V-Mo/HZSM-5 produced, butyric acid and succinic acid together with maleic acid.

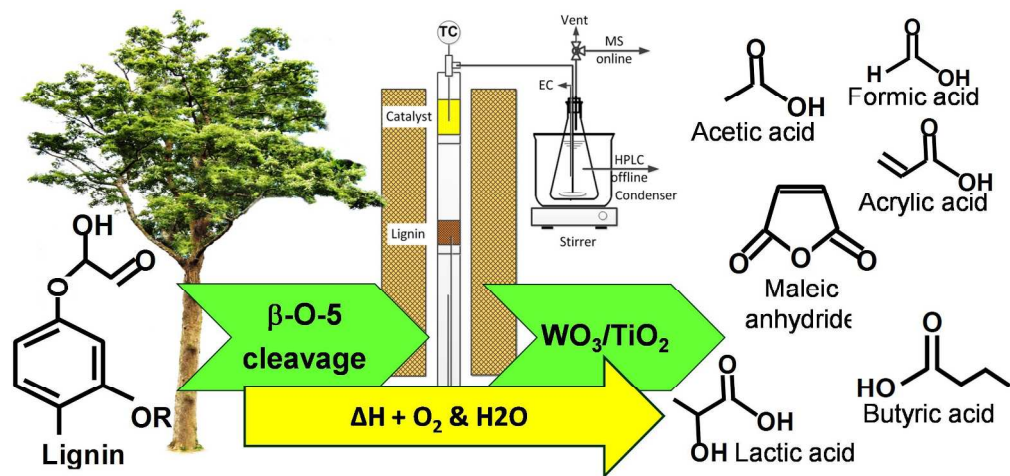
5 Acknowledgements

The authors acknowledge NSERC for financial support and DuPont for supplying the VPP catalyst and FPInnovation for supplying lignin and analytical assistance. In addition, special thanks to NSERC Biomaterials and Chemicals Strategic Network (www.lignowork.ca). We acknowledge NSERC for the Banting post-doctoral fellowship granted to Dr. Boffito. We wish to thank Dr. Amir Saffar from Polytechnique de Montréal for helping with the FTIR analysis.

References

- J. Zakzeski, A. L. Jongerijs, P. C. A. Bruijninx and B. M. Weckhuysen, *ChemSusChem*, 2012, **5**, 1602–1609.
- M. Fan, P. Jiang, P. Bi, S. Deng, L. Yan, Q. Zhai, T. Wang and Q. Li, *Bioresour. Technol.*, 2013, **143**, 59–67.
- A. J. Ragauskas, G. T. Beckham, M. J. Biddy, R. Chandra, F. Chen, M. F. Davis, B. H. Davison, R. A. Dixon, P. Gilna, M. Keller, P. Langan, A. K. Naskar, J. N. Saddler, T. J. Tschaplinski, G. A. Tuskan and C. E. Wyman, *Science*, 2014, **344**, 1246843.
- D. Lalitendu, K. Praveen and S.-S. Ratna, *Biofuels*, 2012, **3**, 155–166.
- R. Ma, Y. Xu and X. Zhang, *ChemSusChem*, 2015, **8**, 24–51.
- D. R. Vardon, M. A. Franden, C. W. Johnson, E. M. Karp, M. T. Guarnieri, J. G. Linger, M. J. Salm, T. J. Strathmann and G. T. Beckham, *Energy Environ. Sci.*, 2015, **8**, 617–628.
- E. Feghali, G. Carrot, P. Thuery, C. Genre and T. Cantat, *Energy Environ. Sci.*, 2015, **8**, 2734–2743.
- S. Van den Bosch, W. Schutyser, R. Vanholme, T. Driessen, S.-F. Koelewijn, T. Renders, B. De Meester, W. J. J. Huijgen, W. Dehaen, C. M. Courtin, B. Lagrain, W. Boerjan and B. F. Sels, *Energy Environ. Sci.*, 2015, **8**, 1748–1763.
- Q. Song, F. Wang, J. Cai, Y. Wang, J. Zhang, W. Yu and J. Xu, *Energy Environ. Sci.*, 2013, **6**, 994–1007.
- A. Rahimi, A. Ulbrich, J. J. Coon and S. S. Stahl, *Nature*, 2014, **515**, 249–252.
- C. Li, X. Zhao, A. Wang, G. W. Huber and T. Zhang, *Journal of Chemical Reviews*, 2015, **115**, 11559–11624.
- P. Azadi, O. R. Inderwildi, R. Farnood and D. A. King, *Renewable and Sustainable Energy Reviews*, 2013, **21**, 506–523.
- A. Witsuthammakul and T. Sooknoi, *Applied Catalysis A: General*, 2012, **413–414**, 109–116.
- X. Xu, J. Lin and P. Cen, *Chinese Journal of Chemical Engineering*, 2006, **14**, 419–427.
- K. Kadowaki, K. Sarumaru and T. Shibano, *Production of acrylic acid US3773828*, 1980.
- M. Kwan, N. Cant, D. Trimm and M. Wainwright, *Applied Catalysis*, 1987, **31**, 25–34.
- Y. Ma, Z. Du, J. Liu, F. Xiaab and J. Xu, *Green Chemistry*, 2015, **17**, 4968–4973.
- C. S. Lancefield and N. J. Westwood, *Green Chem.*, 2015, **17**, 4980–4990.
- M. Brebu and C. Vasile, *Cellulose Chemistry and Technology*, 2010, **44**, 353–363.
- R. N. Olcese, G. Lardier, M. Bettahar, J. Ghanbaja, S. Fontana, V. Carré, F. Aubriet, D. Petitjean and A. Dufour, *ChemSusChem*, 2013, **6**, 1490–1499.
- S. Lotfi, D. C. Boffito and G. S. Patience, *ChemSusChem*, 2015, **8**, 3424–3432.
- W. Mu, H. Ben, A. Ragauskas and Y. Deng, *BioEnergy Research*, 2013, **6**, 1183–1204.
- L. Kouisni, P. Holt-Hindle, K. Maki and M. Paleologou, *Science & Technology for Forest Products and Processes*, 2012, **2**, 6–10.
- L. Kouisni and M. Paleologou, *Method for separating lignin from black liquor US Patent 8771464*, 2014.
- M. Y. Balakshin and E. A. Capanema, *RSC Adv.*, 2015, **5**, 87187–87199.
- S. Constant, H. L. J. Wienk, A. E. Frissen, P. P. de, R. Boelens, D. S. van Es, R. J. H. Grisel, B. M. Weckhuysen, W. J. J. Huijgen, R. J. A. Gosselink and P. C. A. Bruijninx, *Green Chem.*, 2016.
- L. V. Kanitskaya, A. F. Gogotov, D. T. T. Khai and A. V. Rokhin, *Russian Journal of Bioorganic Chemistry*, 2012, **38**, 720–725.
- L. B. Davin, M. Jourdes, A. M. Patten, K.-W. Kim, D. G. Vassao and N. G. Lewis, *Nat. Prod. Rep.*, 2008, **25**, 1015–1090.
- Y. Pu, B. Hallac and A. J. Ragauskas, *Plant Biomass Characterization: Application of Solution- and Solid-State NMR Spectroscopy*, John Wiley Sons, Ltd, 2013, pp. 369–390.
- G. S. Patience and R. E. Bockrath, *Applied Catalysis A: General*, 2010, **376**, 4–12.
- Pingxiang XingFeng Chemical Packing Co., Ltd.
- J. Dubois, C. Duquenne and W. Hoelderlich, *Process for dehydrating glycerol to acrolein*, 2006, WO Patent App. PCT/EP2006/000,735.
- M. Dalil, D. Carnevali, J.-L. Dubois and G. S. Patience, *Chemical Engineering Journal*, 2015, **270**, 557–563.

- 34 V. Lochař and L. Smoláková, *Reaction Kinetics and Catalysis Letters*, 2009, **96**, 117–123.
- 35 M. J. Lorences, G. S. Patience, F. V. Díez and J. Coca, *Industrial & Engineering Chemistry Research*, 2003, **42**, 6730–6742.
- 36 S. Farag, L. Kouisni and J. Chaouki, *Energy & Fuels*, 2014, **28**, 1406–1417.
- 37 M. T. Klein and P. S. Virk, *Energy & Fuels*, 2008, **22**, 2175–2182.
- 38 R. K. Sharma, J. B. Wooten, V. L. Baliga, X. Lin, W. G. Chan and M. R. Hajaligol, *Fuel*, 2004, **83**, 1469–1482.
- 39 M. M. Ibrahim, M. N. Nadiyah and H. Azian, *Journal of Applied Sciences*, 2006, **6**, 292–296.
- 40 S. Neto, H. Hibst, F. Rosowski and S. Storck, *Multimetal oxide containing silver, vanadium and a promoter metal and use thereof*, 2008, US Patent 7,462,727.
- 41 T. Heidemann, F. Rosowski, G. Linden, M. Seufert, G. Hefele and P. M. Lorz, *Method for producing shell catalysts for the catalytic vapor-phase oxidation of aromatic hydrocarbons and catalysts obtained in such a manner*, 2003.
- 42 L. Lloyd, *Handbook of industrial catalysts*, CSpringer, 2011.
- 43 M. Y. H. Kwan, *PhD thesis*, University of New South Wales, 1985.
- 44 B. M. Weckhuysen and D. E. Keller, *Catalysis Today*, 2003, **78**, 25 – 46.
- 45 J. Zakzeski, P. C. A. Bruijninx, A. L. Jongerius and B. M. Weckhuysen, *Chemical reviews*, 2010, **110**, 3552–99.
- 46 A. Chieragato, J. M. L. Nieto and F. Cavani, *Coordination Chemistry Reviews*, 2015, 3–23.
- 47 S. Jia, B. J. Cox, X. Guo, Z. C. Zhang and J. G. Ekerdt, *Industrial and Engineering Chemistry Research*, 2011, pp. 849–855.
- 48 R. S. Barker, *Method of oxidizing benzene to maleic anhydride using a vanadium, molybdenum, boron containing catalyst*, 1975.
- 49 C. Uraz and S. Atalay, *Chemical Engineering Technology*, 2007, **12**, 1708–1715.
- 50 A. L. Jongerius, R. Jastrzebski, P. C. Bruijninx and B. M. Weckhuysen, *Journal of Catalysis*, 2012, **285**, 315–323.
- 51 M. Koyama, *Bioresource Technology*, 1993, **44**, 209–215.
- 52 P. F. Lovell, *AIChE Journal*, 1981, **27**, 316–316.
- 53 C. Fumagalli, G. Golinelli, G. Mazzoni, M. Messori, G. Stefani and F. Trifiró, *F. Trifiró*, 1994, vol. 82, pp. 221 – 231.
- 54 G. Ramis, G. Busca, C. Cristiani, L. Lietti, P. Forzatti and F. Bregani, *Langmuir*, 1992, **8**, 1744–1749.
- 55 G. Centi, *Applied Catalysis A*, 1996, 267–298.
- 56 S. Bagheri, N. M. Julkapli and S. B. A. Hamid, *The Scientific World Journal*, 2014, **2014**, 727496.
- 57 A. Corma and L. Sauvanaud, *Catalysis Today*, 2013, **218-219**, 107–114.
- 58 *Catalysis on the Energy Scene*, Elsevier, 1984, vol. 19, pp. 93–100.
- 59 A. Akbari and S. M. Alavi, *Chemical Engineering Research and Design*, 2015, 286–296.
- 60 H. Chen, M. Tang, Z. Rui and H. Ji, *Industrial and Engineering Chemistry Research*, 1996, 267–298.
- 61 Y. Zhu, M. Shen, Y. Xia and M. Lu, *Catalysis Communication*, 2015, 37–43.
- 62 H. P. Dias, G. R. Goncalves, J. C. Freitas, A. O. Gomes, E. V. R. D. Castro, B. G. Vaz, G. M. F. V. Aquije and W. Romao, *Energy Conversion and Management*, 2014, 326–333.
- 63 Z. D. Yigezu and K. Muthukumar, *Fuel*, 2015, 113–121.
- 64 D. C. Boffito, C. Neagoe, M. Edake, B. Pastor-Ramirez and G. Patience, *Catalysis Today*, 2014, 13–17.
- 65 D. C. Kannan, *PhD thesis*, UMI, 2009.
- 66 C. Bjórgen, *One-pot Conversion of Biomass to Ethylene Glycol, Propylene Glycol and other Polyols over Carbon Supported Tungsten Catalysts*, 2013.
- 67 A. Gutiérrez-Alejandre, J. Ramírez and G. Busca, *Langmuir*, 1998, **14**, 630–639.
- 68 T. Shishido, A. Inoue, T. Konishi, I. Matsuura and K. Takehira, *Catalysis Letters*, 2000, **68**, 215–221.
- 69 L. Liu, F. Cao, T. Yao, Y. Xu, M. Zhou, B. Qu, B. Pan, C. Wu, S. Wei and Y. Xie, *New J. Chem.*, 2012, **36**, 619–625.
- 70 E. Bordes, *Catalysis Today*, 1987, **1**, 499–526.
- 71 X. Wang, H. Li, Y. Fei, X. Wang, Y. Xiong, Y. Nie and K. Feng, *Applied Surface Science*, 2001, **177**, 8–14.
- 72 A. Teimouri, B. Najari, A. Najafi Chermahini, H. Salavati and M. Fazel-Najafabadi, *RSC Adv.*, 2014, **4**, 37679–37686.
- 73 C. A. Chagas, L. C. Dieguez and M. Schmal, *Catalysis Letters*, 2012, **142**, 753–762.
- 74 B. Liu, L. France, C. Wu, Z. Jiang, V. L. Kuznetsov, H. A. Al-Megren, M. Al-Kinany, S. A. Aldrees, T. Xiao and P. P. Edwards, *Chem. Sci.*, 2015, **6**, 5152–5163.
- 75 R. Naouel, H. Dhaouadi, F. Touati and N. Gharbi, *Nano-Micro Letters*, 2011, **3**, 242–248.
- 76 K. G. Bhattacharyya and A. K. Talukdar, *Catalysis in Petroleum and Petrochemical Industries*, Narosa Publishing House, 2005, p. 272.
- 77 W. Smith, A. Wolcott, R. C. Fitzmorris, J. Z. Zhang and Y. Zhao, *J. Mater. Chem.*, 2011, **21**, 10792–10800.
- 78 J. Gierer, E. Yang and T. Reitberger, *Holzforschung*, 1994, **48**, 405–413.
- 79 O. Karlsson, T. Ikeda, T. Kishimoto, K. Magara and Y. Matsumoto, *International symposium of wood and pulp conference, Yokohama*, 1999, **1**, 178–181.
- 80 O. Karlsson, T. Ikeda, T. K. K. Magara, Y. Matsumoto and S. Hosoya, *Journal of Wood Science*, 2000, **46**, 263–265.
- 81 T. Akiyama, T. Sugimoto, Y. Matsumoto and G. Meshitsuka, *Journal of Wood Science*, 2002, **48**, 210–215.
- 82 D. Shao, J. Liang, X. Cui, H. Xu and W. Yan, *Chemical Engineering Journal*, 2014, **244**, 288–295.
- 83 Y. Hamzeh, G. Mortha, D. Lachenal, J. C. Hostachy and C. Calais, *Journal of Wood Chemistry and Technology*, 2006, **2**, 153–164.
- 84 T. Furusawaa, T. Satoa, M. Saitoa, Y. Ishiyamaa, M. Satob, N. Itoha and N. Suzuki, *Applied Catalysis A*, 2007, **327**, 300–310.



658x319mm (96 x 96 DPI)

Graphical Abstract text

- We combine thermo-chemical processes with oxidative catalysis to convert lignin to aliphatic carboxylic acids mainly C₄ acids. Acid selectivity changed with catalyst.